

Capillary and anchoring effects in thin hybrid nematic films and connection with bulk behavior

D. de las Heras

Departamento de Física Teórica de la Materia Condensada, Universidad Autónoma de Madrid, E-28049 Madrid, Spain

Luis Mederos

Instituto de Ciencia de Materiales de Madrid, Consejo Superior de Investigaciones Científicas, Sor Juana Inés de la Cruz, 3, E-28049 Madrid, Spain

Enrique Velasco

Departamento de Física Teórica de la Materia Condensada and Instituto de Ciencia de Materiales Nicolás Cabrera, Universidad Autónoma de Madrid, E-28049 Madrid, Spain

(Received 26 February 2008; revised manuscript received 24 December 2008; published 30 January 2009)

By means of a molecular model, we examine hybrid nematic films with antagonistic anchoring angles where one of the surfaces is in the strong anchoring regime. If anchoring at the other surface is weak, and in the absence of wetting by the isotropic phase, the anchoring transition may interact with the capillary isotropic-nematic transition. For general anchoring conditions on this surface we confirm the existence of the steplike biaxial phase and the associated transition to the linear constant-tilt-rotation, configuration. The steplike phase is connected with the bulk isotropic phase for increasing film thickness so that the latter transition is to be interpreted as the capillary isotropic-nematic transition in a hybrid film.

DOI: 10.1103/PhysRevE.79.011712

PACS number(s): 61.30.Hn, 61.30.Pq, 68.18.Jk

I. INTRODUCTION

Frustration effects associated with confinement of liquid crystals by competing surface fields continue to attract interest. Hybrid nematic cells, where a nematic material is exposed to two surfaces with strong but opposing anchoring tendencies, are commonly used experimentally to determine anchoring properties of substrates [1,2] and may be important in the context of display device technologies, especially in the case of hybrid twist nematic cells [3].

The two configurations observed in hybrid, homeotropic, planar cells are (Fig. 1) (i) a uniform director along the direction favored by the substrate with the highest anchoring energy (U phase) and (ii) linearly rotating director between the two antagonistic surfaces (L phase). Elastic and surface effects play opposite roles and determine the equilibrium director configuration. A confinement-induced anchoring transition, between the L and U phases, is expected for sufficiently thin cells, as shown by Barbero and Barberi [4]. Using elastic theory, these authors obtained a critical film thickness $h_c = K(1/W_2 - 1/W_1)$, with $W_2 < W_1$ surface strengths and K the elastic constant in the one-elastic-constant approximation, below which the stable phase is U . However, a third possible configuration was proposed by Palffy-Muhoray *et al.* [5] (and a few years before by Schopohl and Sluckin [6] in the context of disclination defects), consisting of two contiguous slabs of nematic material with uniform but opposite director orientations, each following the orientation favored by each substrate. Macroscopically the directors in the two slabs cannot be continuously connected, so that elastic theory cannot be used to describe this phase. Instead, the mesoscopic Landau-de Gennes theory was used in Ref. [5]. This phase is called steplike (S) phase (see Fig. 1), but is also known as director-exchange phase, biaxial phase, etc. Galabova *et al.* [7] obtained more complete phase diagrams including the L , U , and S phases, suggesting different scenarios as the pore thickness and surface strengths are varied.

Although the S phase, predicted by the phenomenological Landau-de Gennes theory [5,7,8], has been confirmed by Monte Carlo simulation on a (lattice-spin) Lebwohl-Lasher model [9], no experimental evidence seems to exist as yet (see, however, Ref. [10]), presumably because the step-to-linear (SL) phase transition will take place very close to the bulk isotropic-nematic transition and for a cell thickness of a few tens of nanometers [8], challenging experimental verification. In the theoretical front, the role of the different phases and of the capillary isotropic-nematic transition in the surface phase diagram has not been clearly stated yet. In particular, the analysis of the connection between the surface and bulk behaviors in hybrid cells (in particular, the role played by the surface anchoring transition at a single substrate) is, we believe, still incomplete.

In this article we establish the connection between capillary and anchoring effects, on the one hand, and clarify the role of the SL transition in the surface phase diagram, on the other, in an asymmetric nematic film confined between dissimilar, parallel substrates. These connections have not been

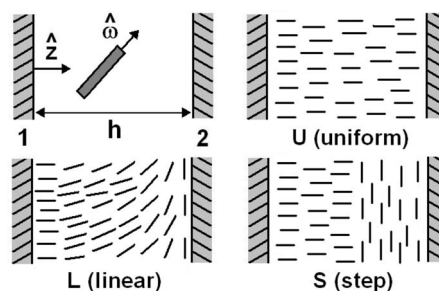


FIG. 1. Geometry used for the calculations and director configurations for the three possible phases inside a hybrid cell. The U phase, here represented with homeotropic orientation, may also have planar orientation, depending on the relative anchoring energies of the two antagonistic substrates.

made, at least fully explicitly, in previous works. In contrast with previous theoretical work based on mesoscopic models, the problem is analyzed using a mean-field molecular theory applied to an athermal fluid of hard anisotropic particles that undergoes an isotropic-nematic transition with respect to chemical potential (which plays the role of an inverse temperature in a thermotropic liquid crystal). The model, extensively tested previously [11,12], consistently describes bulk and interfacial properties, allowing for a microscopically based assessment of the effects of surface interactions, wetting properties, and elastic free energies, on the formation of the S phase. Our analysis indicates that the SL transition corresponds to the usual capillary isotropic-nematic transition, well described, in the limit of thick planar cells, by the Kelvin equation, which relates the transition to the wetting conditions of the substrates. Finally, we relate the capillary transition to the anchoring transition in the confined system when one of the substrates is in the weak anchoring regime.

II. THEORY

The theoretical model is a variation of the density-functional theory of Onsager, with Parsons-Lee (PL) rescaling [13,14], formulated for rigid hard-rod particles (hard spherocylinders) with an aspect ratio $L/D=5$ (L is the length of the cylindrical section while D is the diameter of the two spherical caps at the two ends of the particle). Using Monte Carlo simulation, this hard-particle model has been shown to exhibit stable nematic and smectic phases [15]. In the following, we give a brief presentation of the theory (see Refs. [11,12] for a full account of the theory and its numerical implementation).

In the theory the grand-potential free energy $\Omega[\rho]$ is minimized with respect to the density distribution $\rho(z, \hat{\omega})$, with z the normal distance from the left substrate and $\hat{\omega}$ a unit vector along the main axis of the uniaxial rods, as indicated in Fig. 1 (due to the invariance of the problem in the xy plane, the density distribution is going to depend on the z coordinate only). The expression for the grand-potential free-energy functional per unit area A and unit thermal energy kT is

$$\frac{\beta\Omega[\rho]}{A} = \int_0^h dz \int d\hat{\omega} \rho(z, \hat{\omega}) \left\{ \ln[\rho(z, \hat{\omega})\Lambda^3] - 1 + \frac{\Delta\Psi[\rho(z, \hat{\omega})]}{4\pi\rho(z)\sigma_{\text{eq}}^3} \int_0^h dz' \int d\hat{\omega}' \rho(z', \hat{\omega}') \times V(z-z', \hat{\omega}, \hat{\omega}') - \beta\mu + V_{\text{ext}}(z, \hat{\omega}) \right\}, \quad (1)$$

where, as usual, $\beta=1/kT$, μ is the chemical potential, Λ the thermal wavelength, $\rho(z)$ is the local number density, and σ_{eq} is the diameter of an equivalent hard sphere with the same volume as our spherocylinder. The theory includes interactions from excluded volume effects, contained in the func-

tion $V(z, \hat{\omega}, \hat{\omega}')$ (the excluded area between two hard rods with orientations $\hat{\omega}$ and $\hat{\omega}'$ and centers of mass with relative coordinate z), which promote nematic ordering at high packing fractions, and entropic contributions from orientational degrees of freedom, which play against those effects. In fact this theory is a simplification of a theory proposed by Somoza and Tarazona [16] (ST) which extends the highly successful weighted-density approximation for hard spheres to hard bodies with anisotropic shape using ideas from the PL theory. The simplification of the ST theory, giving rise to Eq. (1), involves approximating the averaged density in the ST theory by the local density distribution $\rho(z, \hat{\omega})$, a procedure which is valid for smoothly varying densities (i.e., far from the region of smectic stability). It is not the purpose of the present article to derive the theory; we only note that the density factor in Eq. (1), $\Delta\Psi(\rho)$, is the excess free energy per particle of a uniform fluid of hard spheres with density ρ (taken from the Carnahan-Starling equation of state), while the denominator $4\pi\rho\sigma_{\text{eq}}^3/3$ is equal to twice the hard-sphere second-virial coefficient of hard spheres multiplied by density. The spatial integrals over the excluded area give twice the second virial coefficient averaged over one particle; therefore this scheme approximates, locally in $(z, \hat{\omega})$, the excess free energy in terms of that of a hard-sphere fluid, which somehow implies a resummation of the whole virial series, but keeping the exact second-order virial coefficient of the actual molecule (containing all of the relevant orientational dependencies), in the spirit of the PL scheme. In the limit of uniform density, the theory strictly coincides with the PL theory.

A bulk isotropic-nematic transition is predicted by the theory, for sufficiently slender rods, at a chemical potential μ_b . When the fluid is in contact with a substrate (or with two substrates, as in the present case), structural quantities depend locally on the position. Four such quantities are needed to describe ordering: $\rho(z)$, the local number density; $\eta(z)$ and $\sigma(z)$, the uniaxial and biaxial nematic order parameters with respect to the local director $\hat{\mathbf{n}}$; and $\psi(z)$, the tilt angle of the local director with respect to the substrate normal along the unit vector $\hat{\mathbf{z}}$. Usually the nematic order parameters are introduced in a laboratory frame, fixed, e.g., to the substrate. This is done by using a Legendre expansion for the orientational distribution function $f(z, \hat{\omega})$, which is defined by $\rho(z, \hat{\omega}) = \rho(z)f(z, \hat{\omega})$ in terms of the one-particle distribution function $\rho(z, \hat{\omega})$ and the local density $\rho(z)$. The expansion reads

$$f(z, \hat{\omega}) = \sum_{lm} \sqrt{\frac{2l+1}{4\pi}} f_{lm}(z) Y_{lm}^*(\hat{\omega}). \quad (2)$$

For particles exhibiting cylindrical and head-tail symmetry the two lowest-order relevant subspaces are $l=0$ and $l=2$. The five coefficients of the subspace $l=2$, i.e., $m=0, \pm 1, \pm 2$, can be reduced to three if one chooses the director to always lie in the xz plane, because of the symmetry of $f(z, \hat{\omega})$ with respect to reflections through this plane. In this case $f_{2,2}=f_{2,-2}$ and $f_{2,1}=-f_{2,-1}$, and the coefficients are

$$\begin{aligned}
 \eta'(z) &\equiv f_{20}(z) = \int d\hat{\omega} f(z, \hat{\omega}) P_2(\hat{\omega} \cdot \hat{\mathbf{z}}), \\
 \sigma'(z) &\equiv \sqrt{\frac{8}{3}} f_{22}(z) = \int d\hat{\omega} f(z, \hat{\omega}) \sin^2 \theta \cos 2\phi, \\
 \nu'(z) &\equiv -\sqrt{\frac{8}{3}} f_{21}(z) = \int d\hat{\omega} f(z, \hat{\omega}) \sin 2\theta \cos \phi, \quad (3)
 \end{aligned}$$

with (θ, ϕ) the polar and azimuthal angles of $\hat{\omega}$. However, it is more intuitive (though not necessarily more advantageous from a computational point of view with the present interaction model) to work in the director frame, where the z axis points along the director. In this frame one has to specify the local tilt angle $\psi(z)$ relating both frames; now there are only two independent nematic order parameters $\eta(z)$, the uniaxial order parameter, and $\sigma(z)$, the biaxial order parameter, which are related locally to the corresponding parameters in the lab frame by

$$\begin{aligned}
 \eta' &= \eta P_2(\cos \psi) + \frac{3}{4} \sigma \sin^2 \psi, \\
 \sigma' &= \eta \sin^2 \psi + \frac{1}{2} \sigma (1 + \cos^2 \psi), \\
 \nu' &= \eta \sin 2\psi - \frac{1}{2} \sigma \sin 2\psi. \quad (4)
 \end{aligned}$$

A description in terms of $\{\eta', \sigma', \nu'\}$ is fully equivalent to a description in terms of the set $\{\eta, \sigma, \psi\}$. Therefore, four independent functions $\rho(z)$, $\eta(z)$, $\sigma(z)$, and $\psi(z)$ are needed to specify the equilibrium configuration of the fluid. Our procedure now involves representing the local orientational distribution function $f(z, \hat{\omega})$ via a convenient parametrization in terms of local effective fields $\Lambda_i(z)$ as follows [11,12]:

$$f(z, \hat{\omega}) = \frac{e^{\Lambda_1(z) P_2(\cos \theta) + \Lambda_2(z) \sin^2 \theta \cos 2\phi + \Lambda_3(z) \sin 2\theta \cos \phi}}{\int d\hat{\omega} e^{\Lambda_1(z) P_2(\cos \theta) + \Lambda_2(z) \sin^2 \theta \cos 2\phi + \Lambda_3(z) \sin 2\theta \cos \phi}}. \quad (5)$$

The local effective fields are related to the local order parameters $\eta(z)$ and $\sigma(z)$ and to the local tilt angle $\psi(z)$ implicitly via Eqs. (3)–(5). This relation is obtained numerically.

In the planar slit the effect of each substrate is accounted for by means of a one-particle external potential $V_{\text{ext}}(z, \hat{\omega})$ which contains two additive parts: $V_{\text{ext}}^{(1)}(z, \hat{\omega})$ for the substrate at left and $V_{\text{ext}}^{(2)}(z, \hat{\omega})$ for the substrate at right (see Fig. 1). They are given by

$$\begin{aligned}
 V_{\text{ext}}^{(1)}(z, \hat{\omega}) &= \begin{cases} \infty, & z < 0, \\ W_1 e^{-\alpha z} P_2(\hat{\omega} \cdot \hat{\mathbf{z}}), & z > 0, \end{cases} \\
 V_{\text{ext}}^{(2)}(z, \hat{\omega}) &= \begin{cases} \infty, & z > h, \\ W_2 e^{-\alpha(h-z)} P_2(\hat{\omega} \cdot \hat{\mathbf{z}}), & z < h, \end{cases} \quad (6)
 \end{aligned}$$

where $P_2(x)$ is a Legendre polynomial. The exponentially decaying external potential is used as a convenient theoretic

cal modelization for actual calculations. It has been used very often in models for the wetting transition in simple fluids [17]. A decaying power-law function, such as z^{-3} , as would be expected from dispersion forces, cannot be said to be more appropriate, given the simplistic level of modelization for interactions considered here. In reality interactions may involve polar, multipolar, solvent-mediated, apart from dispersion, forces, while steric interactions are being approximated by a simple hard-rod force, and molecular flexibility ignored altogether. Therefore we believe that, for a qualitative discussion on director distortion and phase behavior, it is sufficient to keep the model as simple as possible, and Eqs. (6) contain the essential physical ingredients of surface-molecule interactions, i.e., surface strengths W_i and an interaction range α . In all our calculations we set $\alpha = 0.88(L+D)^{-1}$, i.e., the potential range extends up to roughly one particle length (calculations for different values—larger and smaller—have been done with no qualitative changes in the conclusions; note that a power-law function would not allow us to change the range of the interaction as simply as with the exponential function).

Equilibrium values for structural functions are the result of the competition between ideal, hard, and external potential interactions. These equilibrium structures are obtained by numerically minimizing the grand potential density $\Omega[\rho]/A$ with respect to the four structural profiles $\rho(z)$, $\eta(z)$, $\sigma(z)$, and $\psi(z)$ by means of an optimized conjugate-gradient scheme [11,12]. Spatial integrals along z in Eq. (1) are discretized using a step Δz such that a particle length $L+D$ is divided into 30 intervals [i.e., $\Delta z/(L+D) = 0.033$]. This choice gives a good accuracy since the profiles are expected to vary smoothly with z (in fact, smaller values of Δz produce essentially the same results). Angular integrals are discretized in the variables $\hat{\omega} = (\theta, \phi)$, with $\theta \in [0, \pi/2]$, $\phi \in [0, \pi]$ (in both cases the symmetry of the orientational distribution function is exploited), using Gaussian quadratures with 18 roots in both cases. Note that no boundary conditions are imposed on the fluid, the structural functions being completely free at the boundaries and in the rest of the cell. From this point of view and, strictly speaking, the hybrid character of the cell is not fixed since the structure of the fluid within the cell will depend on the thermodynamic conditions imposed on the fluid.

This model has been used [11,12] to explore wetting properties; it also predicts an anchoring transition [11]. Figure 2 is the interfacial phase diagram for a single-substrate system in the $\Delta\mu \equiv \mu - \mu_b$ vs surface strength W plane. The thick lines correspond to regimes of complete wetting by a nematic phase with homeotropic (\perp , line at left) or planar (\parallel , right) director orientations. The anchoring transition for $\Delta\mu \geq 0$ (thin line) separates states with homeotropic orientation from states with parallel orientation of the nematic director. Note that homeotropic states are stable for values of W less than some positive critical value $W = 0.168kT$; this is because a pure hard wall acting on the particle's centers of mass ($W=0$) promotes a perpendicular orientation of the director in an adsorbed layer of nematic material, even though the orientation of single particles would be neutral to this interaction. This is the result of a nontrivial coupling between orientation and packing effects (particles pack more effi-

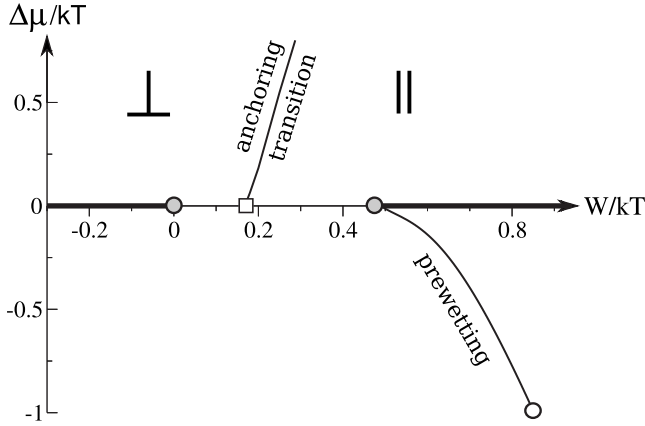


FIG. 2. Interfacial phase diagram of the single-substrate model. $\Delta\mu$ is the chemical potential relative to bulk coexistence and W the surface strength. \perp and \parallel indicate nematic bulk director configurations perpendicular (homeotropic) and parallel to substrate, respectively. Thick lines indicate complete wetting regimes, bounded by wetting transitions (gray circles). Thin lines are anchoring and prewetting transitions for substrate 2, terminating respectively in anchoring transition at bulk coexistence (square) and prewetting critical point (open circle).

ciently when in perpendicular orientation, even in the presence of a weak external field $0 < W < 0.168kT$ that promotes parallel surface orientation). A truly hard wall (acting on the whole particle surface and not simply on the centers of mass) would not exhibit this effect.

In the calculations for a confined system that follow, substrate 1 will always be taken to be in the regime of complete wetting by nematic with homeotropic orientation \perp (i.e., $W_1 \leq 0$) and in the strong anchoring case (i.e., sufficiently far from the anchoring transition line), while the state of substrate 2 will be chosen in the regimes of complete wetting or partial wetting (i.e., with W_2 larger and less than $0.478kT$ —the location of the wetting transition—respectively), but with planar orientation \parallel . In the latter case (i.e., that of partial wetting), proximity to the anchoring transition (as μ is increased from the bulk value μ_b) implies a regime of weak anchoring, and this will bring about interaction of anchoring and capillary effects in the confined system. Note that the wetting transition in the case of planar orientation is of first order, and an associated prewetting transition occurs in the

isotropic part of the phase diagram ($\Delta\mu < 0$). The model does not predict a region of wetting by the isotropic phase; consequently, we expect no suppression of the capillary isotropic-nematic transition [18,19] in our system.

III. RESULTS

As mentioned above, we consider the case where one of the substrates is always in the strong anchoring regime (substrate 1), while the other substrate (2) may be in the strong or weak regime; in both situations the favoured anchoring angle at substrate 1 is homeotropic, and that at substrate 2 planar. We deal with the two situations separately.

A. Strong anchoring in both substrates

Our first result is Fig. 3(a), which depicts the surface phase diagram in the $\Delta\mu$ vs film thickness h plane. Conditions of wetting by nematic and strong anchoring with homeotropic and planar alignments in substrates 1 and 2, respectively, are imposed; therefore no anchoring transition is expected in the nematic region. The line represents a first-order SL phase transition separating two confined structures, the L and S phases. For thin films the line terminates in a critical point. Therefore, the stable director configuration for sufficiently thin films is the S phase (as predicted by Palffy-Muhoray *et al.* [5]), but only below the transition line (provided the latter is within the stable nematic region and that no spatially ordered phases are stabilized).

What is the structure of the L and S phases? This is shown in Fig. 4, where the density and order parameter profiles of the two structures coexisting at point p [panels (a)–(d)] and point q (e)–(h) on the transition line depicted in Fig. 3(a) are shown. The local densities of the two structures are rather similar, except for a slight density depletion in the central region of the cell in the case of the S phase. The tilt-angle profiles already indicate a dramatically different arrangement of the director field in the cell in the S and L phases: in the first the profile changes abruptly in the central region [Fig. 4(b)], while in the second it varies smoothly. Particularly interesting is the behavior of η for the S phase in this region at point p ; it drops almost to zero symmetrically with respect to the step position, Fig. 4(c). A similar profile was presented by Sarlah and Zumer [8] using Landau theory, except for a smoother behavior at the step and the absence of structure

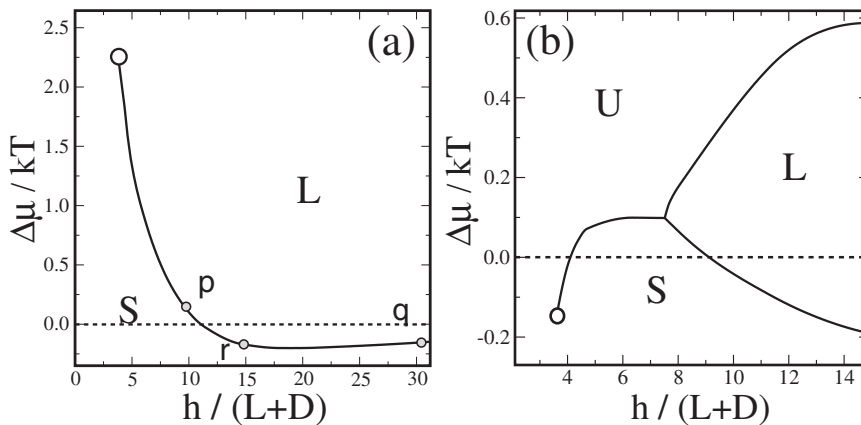


FIG. 3. Interfacial phase diagram in the chemical potential $\Delta\mu$ vs pore width h plane, for values of the surface strengths (a) $W_1 = -1kT$, $W_2 = 3kT$ and (b) $W_1 = 0$, $W_2 = 0.35kT$. Points p and q in (a) are the two coexistence points for which order-parameter and tilt-angle profiles are shown in Fig. 4, while profiles at point r are shown in Fig. 5 (see text for discussion). Open circles are surface critical point.

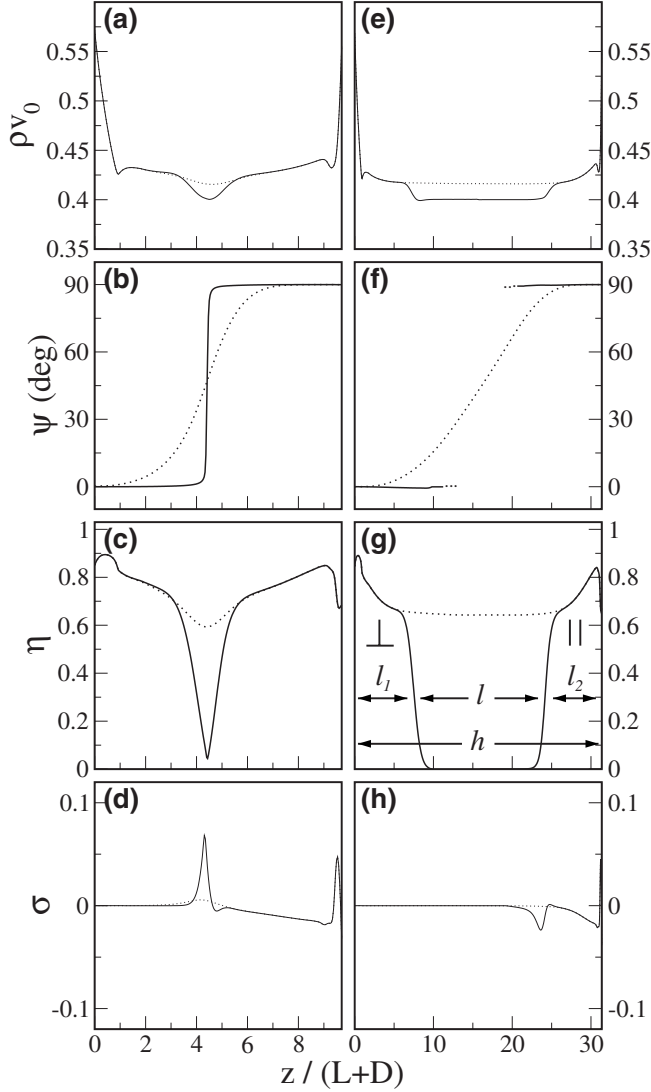


FIG. 4. Local density $\rho(z)$ (scaled with particle volume v_0), tilt-angle $\psi(z)$ (in degrees), uniaxial order-parameter $\eta(z)$, and biaxial order-parameter $\sigma(z)$ profiles for the two film structures that coexist at points p [panels (a), (b), (c), and (d)] and q [panels (e), (f), (g), and (h)] in the phase diagram of Fig. 3(a). Continuous line: S phase; dotted line: L phase. In (f) the tilt angle profile in the isotropic region is not plotted since it cannot be defined. The various thicknesses defined in the text are indicated in panel (g).

near the substrates walls. This is understandable in view of the mesoscopic nature of their theory. The maxima next to the substrates, visible in our profile, are peculiar to the external field used and have been observed also in computer simulations [21,22].

One can interpret these structural profiles as indicating the presence of a planar defective region sandwiched between two finite-thickness nematic films with opposite director orientations, i.e., a “true” S phase. However, in the S -type structure of point q [Fig. 4(g)], a structure thermodynamically connected with the corresponding structure at point p , this region has evolved into a well-developed isotropic slab whose thickness l depends on the departure from the bulk $\Delta\mu$. If l_1 and l_2 are the thicknesses of the incipient wetting

nematic layers, then [see Fig. 4(g)] $l = h - l_1 - l_2 \sim |\Delta\mu|^{-1}$ according to Kelvin equation (see below). It follows that l is an increasing function of h as $h \rightarrow \infty$ for the coexisting S phase and, for large values of h , the isotropic slab completely decouples the two nematic films with opposite director orientations [23], the situation being identical to the usual capillary isotropic-nematic transition in symmetric or nearly symmetric cells. Therefore, the S phase is in fact a confined phase connected with the bulk isotropic (I) phase, whereas the L phase corresponds to the confined phase connected with the bulk nematic (N) phase: we are observing the usual capillary IN transition line.

As $h \rightarrow \infty$ (thick films) the transition line approaches the bulk value μ_b from below, as corresponds to a preference of the substrate for the nematic phase. The nonmonotonic shape of the transition line can be understood from a competition between capillary and elastic effects in the L phase [9]. A simple macroscopic analysis, identical to that leading to the Kelvin equation for confined liquid crystals [20] but including elasticity, can be made as follows. The free energy per unit area A of the confined isotropic and nematic phases are

$$\frac{\Omega_I}{A} = \gamma_{WI}^{\parallel} + \gamma_{WI}^{\perp} + \omega_b^{(I)}h - \rho_b^{(I)}h\Delta\mu,$$

$$\frac{\Omega_N}{A} = \gamma_{WN}^{\parallel} + \gamma_{WN}^{\perp} + \omega_b^{(N)}h - \rho_b^{(N)}h\Delta\mu + \frac{F_e}{A}, \quad (7)$$

where $\omega_b^{(I)} = \omega_b^{(N)}$ are the grand free-energy densities at bulk, ρ_b^I, ρ_b^N the corresponding number densities

$$F_e = \frac{1}{2}K \int_V d\mathbf{r} \left(\frac{\partial\psi}{\partial z} \right)^2 = \frac{AhK}{2} \left(\frac{\pi}{2h} \right)^2 = \frac{\pi^2 AK}{8h} \quad (8)$$

is the elastic contribution in the nematic phase, with K the splay elastic constant, and $\gamma_{WI}^{\parallel}, \gamma_{WI}^{\perp}, \gamma_{WN}^{\parallel}$, and γ_{WN}^{\perp} the surface tensions of the substrate-isotropic (WI) and substrate-nematic (WN) interfaces corresponding to planar and homeotropic director configurations. Making $\Omega_I = \Omega_N$ and solving for $\Delta\mu$ leads to the following dependence of the transition line with cell thickness:

$$\Delta\mu(h) = \frac{a_2}{h^2} - \frac{a_1}{h}, \quad a_1 = \frac{\gamma_{WI}^{\parallel} - \gamma_{WN}^{\parallel} + \gamma_{WI}^{\perp} - \gamma_{WN}^{\perp}}{\Delta\rho_b} > 0,$$

$$a_2 = \frac{\pi^2 K}{8\Delta\rho_b} > 0, \quad (9)$$

where $\Delta\rho_b = \rho_b^{(N)} - \rho_b^{(I)}$. As $h \rightarrow \infty$ capillary effects [second term in $\Delta\mu(h)$] dominate and $\Delta\mu(h) \rightarrow 0^-$, but in the thin-film regime elastic effects are more important and $\Delta\mu$ becomes positive. Note that under wetting conditions the capillary term should be $-a_1/l$, but this does not change the argument.

In passing, we comment on the biaxiality profiles $\sigma(z)$ presented in Figs. 4(d) and 4(h). This quantity measures biaxiality with respect to the local director (not with respect to a lab fixed frame), i.e., departures from isotropicity about the local director. Obviously σ is zero or very small when the director is perpendicular to the interfaces, but it becomes

nonzero at the defective central region of the S phase and at the right substrate (where the director is parallel to the substrate plane). Our theory predicts that biaxiality is always significant at the right substrate, and also at the central region in the S phase. In view of this, we can name the S phase the “biaxial” phase, but not because of the obvious rotation of the director by approximately 90° between the two substrates (which establishes two perpendicular axes in the nematic film), since this property holds in both the L and S phases, but because the local biaxiality $\sigma(z)$ is not small in the S phase. Note, however, that biaxiality is not negligible at the isotropic- \parallel nematic interface in the L phase, Fig. 4(h). Sarlah and Zumer [8], in their Landau analysis, also predict biaxiality at the planar defect in the S phase, but not near the two substrates, where order is always uniaxial.

From the results presented so far, we conclude that the S phase is not a genuine phase different from the confined I phase: whether the two nematic films are in contact or not will depend on conditions such as wetting strength and departure from bulk coexistence (determining film thickness) of the particular material or surface. What we can say is that the optimum conditions to observe a “true” S phase, with an intervening defective region of a few molecular widths in thickness and with a tilt angle that changes abruptly (see Fig. 1), involve conditions of complete wetting by nematic at both substrates, sufficiently narrow pore widths and sufficiently developed nematic layers adsorbed at the two substrates (or, equivalently, closeness to the bulk phase transition). Both conditions may play against univocal experimental verification.

Some of these observations are implicit in the recent paper by Chiccoli *et al.* [9] who performed Monte Carlo simulations on a (lattice) Lebwohl-Lasher model. For example, they observe the presence of a “true” S phase (called “biaxial” by Chiccoli *et al.*) for narrow cells and, for off-coexistence thicker cells, they obtain structures where a thick isotropic central region is sandwiched between two nematic films with opposite director orientation. In the latter cases Chiccoli *et al.* assume that, as the transition is approached, the thickness of the isotropic slab decreases and that, right at the transition, the isotropic region has a vanishing thickness. They conclude that, in these cases, the S phase has a negligible stability range and that there exists a maximum cell thickness h_m in which the S phase can be found, which they estimate from the condition $\Delta\mu(h_m)=0$ (i.e., when the extrapolated transition line crosses the bulk transition). Our results suggest that (i) the structural SL transition actually continues to bulk ($h \rightarrow \infty$) as the true capillary isotropic-nematic transition; (ii) strictly speaking, the S phase can be found for any value of cell thickness since, as h is increased, it develops smoothly (i.e., on the same thermodynamic free-energy surface) from the “true” S phase obtained for narrow cells, and (iii) wetting properties, along with closeness to bulk transition and pore width, determine the thickness of the isotropic slab and, therefore, the range of cell widths where the “true” steplike phase can be observed.

As a consequence, the upper cell thickness h_m defined by Chiccoli *et al.* from the condition $\Delta\mu(h_m)=0$ would have, strictly speaking, no special meaning. In fact, for strongly wet substrates, the true S phase could be observed in the

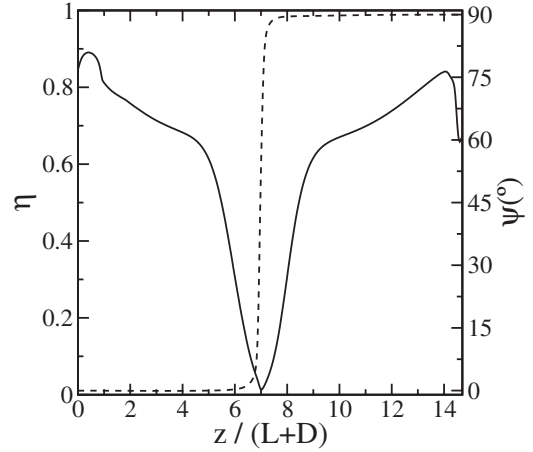


FIG. 5. Uniaxial order-parameter $\eta(z)$ [continuous line] and tilt-angle $\psi(z)$ [dashed line] profiles for a S phase coexisting with a corresponding L phase at a cell thickness $h=14.7(L+D)$ [point r in the phase diagram of Fig. 3(a)].

isotropic region of the phase diagram ($\mu < \mu_b$), although close to the bulk coexistence condition. In Fig. 5 the uniaxial order-parameter and tilt-angle profiles for the S phase coexisting with a L phase are plotted for the case $h=14.7(L+D)$ [point r in the phase diagram of Fig. 3(a)]; the corresponding undersaturation $\Delta\mu < 0$ is close to the maximum one (in absolute value), which occurs when $h \approx 18(L+D)$. We can see that the structure inside the cell is still steplike. The evolution of the thickness of the central isotropic film l , along the transition line, which can be taken as an indication of how far the S phase is from being “genuine,” is plotted in Fig. 6 (l is defined as the distance between the half-height location of the two isotropic-nematic interfaces with respect to the bulk uniaxial nematic order parameter). Clearly two growth régimes are visible: In the first, the width of the central defect remains within one particle length, while in the other the gap

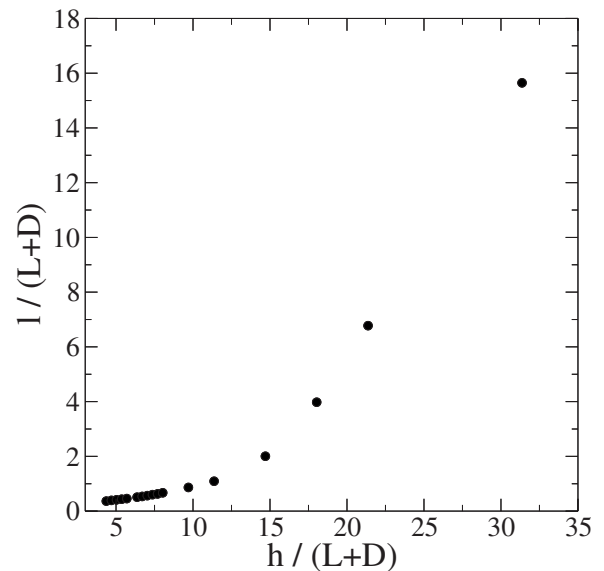


FIG. 6. Thickness l of the isotropic slab as a function of the total cell thickness h (see text for a definition of l).

opens up more or less linearly with h , leaving a thick region of isotropic phase. We might loosely identify the first regime with the true step phase. A more sensible criterion for estimating h_m , based on the change of growth regime gives, from Fig. 6, $h_m \approx 12-14(L+D)$, which for 8CB (with a molecular length ~ 2.2 nm) is equal to ~ 28 nm.

B. Weak anchoring in one of the substrates

Another result of our analysis is that, in the weak anchoring regime of one of the substrates, the SL transition line may in some cases interact with the anchoring phase transition occurring in the semiinfinite case. In our model, the anchoring transition in substrate 2 becomes a UL phase transition in the confined system (with uniform homeotropic orientation in the U phase), but this transition is genuinely different from the SL transition; the two can be present at the same time and may in fact interact in the regime of very narrow pores. This is illustrated in Fig. 3(b), which shows the phase diagram for a case pertaining to substrates with conditions of complete and partial wetting by nematic, respectively, but with an anchoring transition occurring in the latter substrate. In this case a ULS triple point appears.

IV. DISCUSSION AND CONCLUSION

Rodríguez-Ponce *et al.* [24,19] have analyzed a related system using a simplified version of density-functional theory. However, their system is crucially different in that the isotropic phase wets the substrate that undergoes the anchoring transition; the result is that the capillary isotropic-nematic phase transition is suppressed, and capillary and anchoring transitions never occur at the same time in the weak

anchoring regime: no interaction between the two is possible. For the same reason, the U phase is never stabilized and the transition in the confined system always proceeds between the S and L phases. Suppression of the capillary transition is expected whenever the isotropic phase preferentially adsorbs on (or wets) one of the substrates [19] (so that one of the nematic phases, either homeotropic or planar, becomes irrelevant) or the director orientation of the planar nematic film is random [18], the phenomenology being similar to that in magnetic systems [25] (with some variations related to elastic effects).

In summary, we have presented a scenario, based on a microscopic model, for the phase equilibria of a liquid-crystal film subject to opposite anchoring energies in a planar cell. The different possible director structures, their phase boundaries and their relation to the bulk and anchoring transitions of the corresponding system adsorbed on a single substrate, have been discussed. Our theoretical approach is not necessarily superior to previous models based on phenomenological theories. However, we believe that our work clarifies recent analyses on hybrid cells, based on Landau-de Gennes theory, Monte Carlo simulation on a lattice spin model, and density-functional theory, by identifying the structural SL transition as the capillary nematization transition, and also by establishing a link with anchoring phenomena.

ACKNOWLEDGMENTS

We acknowledge financial support from Ministerio de Educación y Ciencia (Spain) under Grant Nos. FIS2005-05243-C01-01 and FIS2007-65869-C03-01, and Comunidad Autónoma de Madrid (Spain) under Grant No. S-0505/ESP-0299.

-
- [1] L. M. Blinov, D. B. Subachyus, and S. V. Yablonsky, *J. Phys.* II **1**, 459 (1991).
- [2] A. Mazzulla, F. Ciuchi, and J. R. Sambles, *Phys. Rev. E* **64**, 021708 (2001).
- [3] F. Bisi, E. C. Gartland, R. Rosso, and E. G. Virga, *Phys. Rev. E* **68**, 021707 (2003).
- [4] G. Barbero and R. Barberi, *J. Phys. (Paris)* **44**, 609 (1983).
- [5] P. Palfy-Muhoray, E. C. Gartland, and J. R. Kelly, *Liq. Cryst.* **16**, 713 (1994).
- [6] N. Schopohl and T. J. Sluckin, *Phys. Rev. Lett.* **59**, 2582 (1987).
- [7] H. G. Galabova, N. Kothekar, and D. W. Allender, *Liq. Cryst.* **23**, 803 (1997).
- [8] A. Sarlah and S. Zumer, *Phys. Rev. E* **60**, 1821 (1999).
- [9] C. Chiccoli, P. Pasini, A. Sarlah, C. Zannoni, and S. Zumer, *Phys. Rev. E* **67**, 050703(R) (2003).
- [10] The S phase may have been observed already in the recent surface-force-apparatus measurements of Zappone *et al.* [B. Zappone, Ph. Richetti, R. Barberi, R. Bartolino, and H. T. Nguyen, *Phys. Rev. E* **71**, 041703 (2005)], who probed nematic films under homeotropic or planar hybrid conditions. At very short film thicknesses (<10 nm) the force between the surfaces becomes strongly attractive, a signature that, according to the authors, may point to a film reconstruction into a steplike phase.
- [11] D. de las Heras, L. Mederos, and E. Velasco, *Phys. Rev. E* **68**, 031709 (2003).
- [12] D. de las Heras, E. Velasco, and L. Mederos, *J. Chem. Phys.* **120**, 4949 (2004).
- [13] J. D. Parsons, *Phys. Rev. A* **19**, 1225 (1979).
- [14] S.-D. Lee, *J. Chem. Phys.* **87**, 4972 (1987).
- [15] P. Bolhuis and D. Frenkel, *J. Chem. Phys.* **106**, 666 (1997).
- [16] A. M. Somoza and P. Tarazona, *Phys. Rev. Lett.* **61**, 2566 (1988).
- [17] D. E. Sullivan and M. M. Telo da Gama in *Fluid Interfacial Phenomena*, edited by C. A. Croxton (Wiley, Chichester, 1986).
- [18] J. Quintana and A. Robledo, *Physica A* **248**, 28 (1998).
- [19] I. Rodríguez-Ponce, J. M. Romero-Enrique, and L. F. Rull, *J. Chem. Phys.* **122**, 014903 (2005).
- [20] A. Poniewierski and T. J. Sluckin, *Liq. Cryst.* **2**, 281 (1987).
- [21] The shifted maxima in the uniaxial order-parameter profile is due to the fact that particles right at the wall have more freedom to orient than particles a bit displaced from the wall, since

orientational motion in the latter is hampered both by the former and by neighbor particles in the outward direction from the wall.

[22] M. P. Allen, *Mol. Phys.* **96**, 1391 (1999).

[23] In our system anchoring at the free isotropic-nematic interface is planar, and the homeotropically oriented nascent wetting nematic film will change to a linearly distorted configuration, with a faster growth rate (from logarithmic to power law) on approaching coexistence; of course, this does not invalidate our argument. See D. E. Sullivan and R. Lipowsky, *Can. J.*

Chem. **66**, 553 (1988); T. J. Sluckin and A. Poniewierski, *Mol. Cryst. Liq. Cryst.* **179**, 349 (1990); F. N. Braun, T. J. Sluckin, and E. Velasco, *J. Phys.: Condens. Matter* **8**, 2741 (1996).

[24] I. Rodríguez-Ponce, J. M. Romero-Enrique, and L. F. Rull, *Phys. Rev. E* **64**, 051704 (2001).

[25] F. Brochard-Wyart and P. G. de Gennes, *C. R. Seances Acad. Sci., Ser. 2* **297**, 223 (1983); A. O. Parry and R. Evans, *Phys. Rev. Lett.* **64**, 439 (1990); M. R. Swift, A. L. Owczarek, and J. O. Indekeu, *Europhys. Lett.* **14**, 475 (1991); for more recent references see, e.g., Ref. [18].